14th IEA Heat Pump Conference
15-18 May 2023, Chicago, Illinois

Flow Boiling Heat Transfer Performance of R448A inside Multiports Mini-Channel tubes with different geometry

Hoang Ngoc Hieu[a], Nurlaily Agustiarini[a], Jong-Taek Oh[b*], Jong Kyu Kim[c]

[(a)] Department of Refrigeration and Air-Conditioning Engineering, Graduate School, Chonnam National University Yeosu, 59626, South Korea
[(b)] Department of Refrigeration and Air-Conditioning Engineering, Chonnam National University, Yeosu, 59626, South Korea
[(c)] Department of Naval Architecture & Ocean Engineering, Chonnam National University, Yeosu, 59626, South Korea

Abstract

R448A, a zeotropic blend with GWP of 1390, is being proposed as an alternative refrigerant working in air-conditioning and heat pump systems. Despite being suitable as drop-in refrigerants, some redesigning of R448A systems was recommended for achieving maximum efficiency. In the work, the heat transfer coefficient of R448A inside multiple multiport mini-channel tube with different geometries were experimentally investigated. The experimental range of mass flux is from 100 to 500 kg/m^{2}s, heat flux from 3 to 15 kW/m^2 at a fixed saturated temperature of 6^{o}C, in 3 multiport tubes with varying hydraulic diameter, number of ports and aspect ratio. The influence of mass flux, heat flux, and vapor quality are examined, as well as the effect of channel geometry on the heat transfer performance. Finally, a correlation including the channel geometrical effect is proposed for the prediction of R448A heat transfer coefficient.

Selection and/or peer-review under the responsibility of the organizers of the 14th IEA Heat Pump Conference 2023.

Keywords: multiport mini-channels;flow boiling; heat transfer coefficient;correlatio;, R448A

1. Introduction

The HVAC industry have been rushing in research and development toward the 4th generation of refrigerant. Ultra-low GWP HFOs blend are currently considered best candidate as they can reduce GWP while retaining a good system performance. R448A is among those candidates, which is a zeotropic blend of 5 different components, consisting of R32, R125, R134a and the HFO's R1234ze and R1234yf. With non-flammability, non-toxicity (safety class A1), and a GWP of 1387, which is over 60% lower in GWP than R404A, it intended replacement, R448A has met many requirements of a high priority candidate.

Theoretical evaluation by Mota-Babiloni et al. [1] of alternative refrigerant with R404A as a baseline considered R448A (N-40) to be the best option in term of energy efficiency among 6 candidates in application which non-flammability is required. Past retrofit testing of R448A in different systems has also been available with the experimental work by Mota-Babiloni et al. [2], which tested R448A and compared against R404A in vapor compression systems. They found R448A charged systems to have lower mass flow rate, cooling capacity, power consumption and higher COP than R404A. The authors considered R448A to be a good alternative for R404A for medium temperature (food conservation) application, and warm climate countries would benefit from R448A due to it higher discharge temperature.

Investigation of R448A flow boiling heat transfer has been available within literatures. Lilio et al [3] experimentally measured R448A heat transfer coefficient and pressure drop in a 6mm steel tube. Heat transfer degradation observed at the mass flux of 150 kg/m^{2}s, which was attributed due to flow stratification. The higher mass flux shows convective behavior, with the heat transfer coefficient increases with quality. Heat flux does

* Corresponding author. Tel.: +82-61-659-7273, fax: +82-61-659-7279.
E-mail address: ohjt@chonnam.ac.kr

not only increase the heat transfer coefficient but also change the data trend with quality and dry-out characteristic. Kim & Kim [4] investigated the heat transfer coefficient and pressure drop of 4 different alternative refrigerants of R404A inside a smooth tube, the interims (R448A, R449A) and long-terms (R455A and R454C) in a smooth tube. At lower mass flux (100 kg/m^{2}s) and low vapor quality at the high mass flux of 300 kg/m^{2}s, R404A heat transfer coefficient is larger than the alternative refrigerant, due to the heat transfer penalization from the alternatives larger temperature glide. However, at the high mass flux of 300 kg/m^{2}s and high vapor quality, R404A heat transfer coefficient is exceeded by the alternative refrigerants, due to their more favorable thermos-physical properties. By the same author, Kim & Kim [5] studied those same blends heat transfer coefficient and pressure drop but in multiport mini-channel tube. Here the heat transfer coefficient of R404A is higher than all of the alternatives. At lower mass flux of 200 kg/m^{2}s, heat transfer coefficient of the alternatives is higher than the interim, while the reverse is true at 400 kg/m^{2}s. Like in Kim & Kim [6], the finding was attributed to the relationship between temperature glide and thermos-physical properties.

A literature survey shows that although R448A is a relatively well research blend recently, their database for multiport mini-channel tube should be supplemented with further data, for better consideration when applying to refrigeration or heat pump systems. Up to date, only Kim & Kim [4] had investigated heat transfer coefficient and pressure drop of R448A inside multiport mini-channel, albeit with only one channel. The current work extends the data for various different channels with varying geometry. The experimental range of mass flux is from 100 to 500 kg/m^{2}s, heat flux from 3 to 15 kW/m^2 at a fixed saturated temperature of 6^{o}C, in 3 multiport tubes with varying geometry. The effect of mass flux, heat flux as well as channel geometry are discussed. Finally, correlations are examined and new one proposed for practical prediction.

2. Experimental Apparatus and Methodology

2.1. Experimental Apparatus

The investigation is carried out through a testing apparatus shown in the following schematic diagram 1.

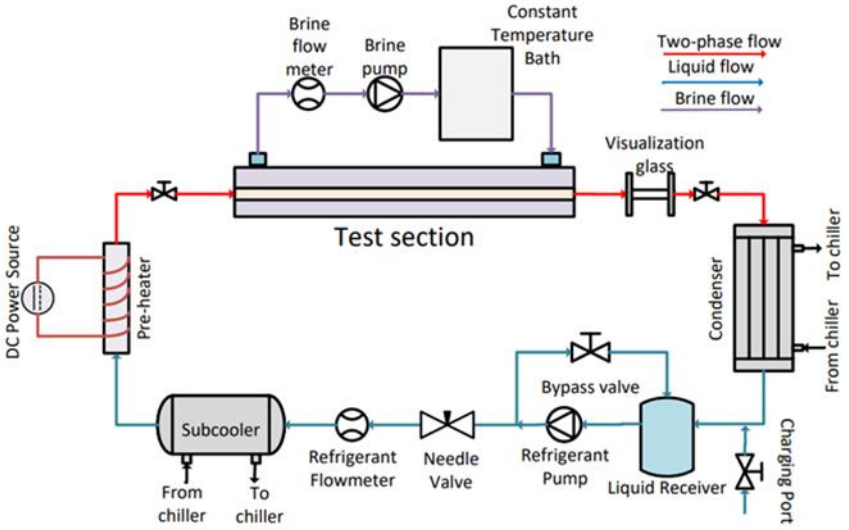

Fig. 1. Experimental systems.

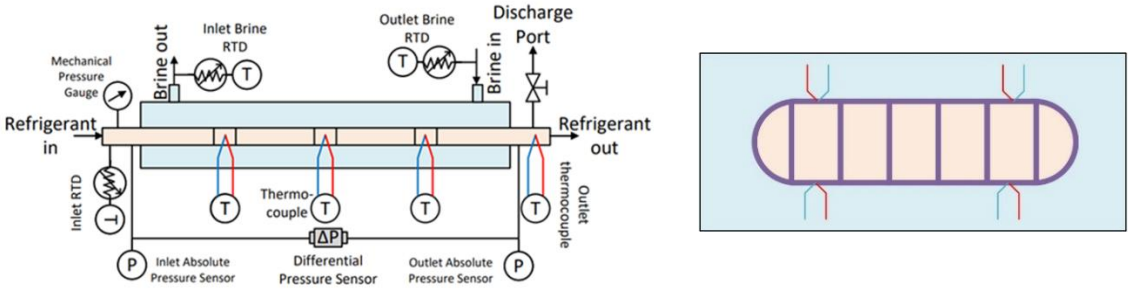

Fig. 2. Test section in detail and layout of thermocouple attachment

The refrigerant micro-gear pump is the driving force of flow circulation. The mass flow rate can be varied using an inverter controlled, while measurement is done by a flow meter installed after the pump. Heating was provided via preheater section, which is a 4m length tube wired to a DC power source. The DC power source power output can be controlled up to 1500W, so as to heat refrigerant up to desired quality before entering the test section, where the measurement of heat transfer coefficient and pressure drop took place. Outlet of the test section is the condenser, where the refrigerant return to liquid phase for next circulation. Refrigeration load for both condenser and sub-cooler come from a chilled brine bath, which is chilled by a separated chiller system. All sensor from the systems is connected to a data-logger then onto a PC for monitoring and recording of data.

Heating for the test section is provided from a warm brine bath. The test section is a counter current heat exchanger, with two acrylic slab sealed a multiport mini-channel tube in the middle. The brine pump was also connected to an inverter controlled to varying the mass flow rate, and a flow meter of same type is used for the measurement of it. Inlet and outlet temperature of the test section are both measured by RTDs, and is used along with mass flow meter for the calculation of applied heat flux. The pair of inlet temperature RTD and inlet absolute pressure transducer is used together to determine the inlet condition (vapor quality and enthalpy). The pressure drop is monitored with a differential pressure sensor, connected from 2 ports from the inlet and outlet of the test section. In order to calculate the heat transfer coefficient, the wall temperature was measured using thin thermos-couples wire. In total 12 was embedded at the surface, in 3 different positions from the inlet, 2 on top and 2 down the bottom in each position, as it is shown in figure 3.

The geometry of testing tube in table 1.

Table 1. Geometrical configuration of test tubes

Tube	H	W	d_h	AR	n
B	2	0.77	1.14	0.345	11
D	1.4	0.87	1.07	0.56	16
E	1.42	0.7	0.969	0.493	9

2.2. Data reduction

With inlet temperature and inlet pressure, it is possible to deduce the vapor quality and enthalpy at the inlet.

$$x_{in} = f(T_{in}, P_{in}), i_{in} = f(T_{in}, P_{in}) \tag{1}$$

The heat flux can be calculated using the brine inlet, outlet temperature and the brine mass flow rate

$$q = \frac{m_{water} C_{p,water} \left(T_{water,in} - T_{water,out}\right)}{A_{ext}} \tag{2}$$

Assuming an even distribution of heat flux across the tube, the enthalpy of i^{th} measurement point can be calculated as follow:

$$i_i = i_{in} + \frac{qP_{tube}}{m_{ref}} z_i \tag{3}$$

Likewise, assuming linear pressure drop, the pressure at the i^{th} measurement point can be calculated as

$$P_i = P_{in} - \Delta P \frac{z_i}{L} \tag{4}$$

With both pressure and enthalpy, it is possible to infer the saturated temperature at that location:

$$T_{sat,i} = f(P_i, i_i) \tag{5}$$

The internal wall temperature can be readily calculated with one dimensional thermal conduction equation through wall. Generally, the difference between internal and external wall temperature is insignificantly small due to the thin wall. The wall temperature is the average temperature of the 4 thermocouples

$$T_{w,in_i} = T_{w,out_i} + \frac{qD}{k} \tag{6}$$

Finally, the heat transfer coefficient can be calculated with the internal wall temperature and the corresponding saturated temperature.

$$h_i = \frac{A_{ext}}{A_{int}} \frac{q}{T_{w,in_i} - T_{sat,i}} \tag{7}$$

The average uncertainty for heat transfer coefficient is roughly 15.4%, while for vapor quality it is kept small at about 0.02.

3. Result and Discussion

3.1. Heat transfer coefficient result

Figure 3 displays the effect of mass flux on the heat transfer coefficient.

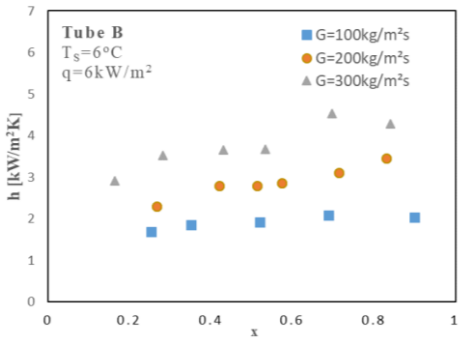

Fig. 3. The effect of mass flux on heat transfer coefficient.

As shown increase the mass flux increases the heat transfer coefficient. The current trend is universal within literature. The contribution of convective boiling in flow boiling heat transfer coefficient is mainly driven by mass flux. With increase mass flux, the annular regime is expanded due to strong inertia of vapor phase. Under annular flow, thin film evaporation occurring at the interface is driven significantly by the effect of interfacial shear stress, which increases along with mass flux. Additionally, an increase in mass flux will decrease the thermal resistance between the liquid film and the vapor core by enhancing the effective turbulent thermal conductivity. Improved turbulent effect at high velocity also help to offset the effect of mass transfer resistance on heat transfer of mixture by improving compositional mixing, as mentioned in Li [6] or Berto [7].

Figure 4 displays the effect of heat flux on the heat transfer coefficient.

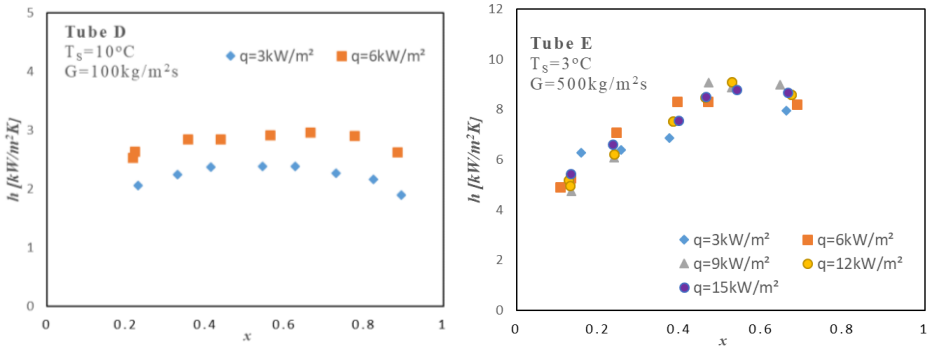

Fig. 4. The effect of heat flux on heat transfer coefficient.

Heat flux affects heat transfer coefficient differently, as it is more dependable on the specific mass flux condition. As explained in conventional nucleate boiling theory as well as being well reported in literature,

increasing heat flux activate more nucleate site and hasten the bubble nucleation and growth cycle, overall enhancing convective boiling. However, with an increasing of mass flux, convective boiling become a dominate flow boiling mechanism, owning to strong effect of interfacial shear and turbulent. Consequently, the effect of heat flux become less noticeable at high mass flux.

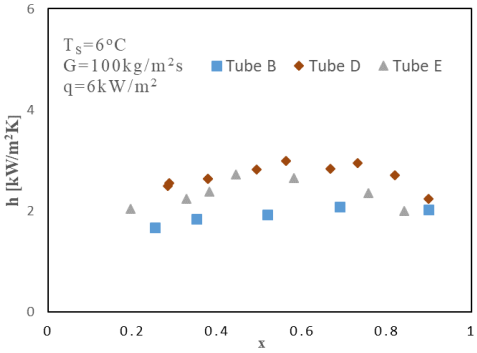

Fig. 5. Heat transfer coefficient comparison between different channels.

Evidently, at lower mass flux condition, where nucleate boiling have more noticeable effect on heat transfer, the heat transfer coefficient follows the descending order of B, D and E. From table 2, the heat transfer was found to generally increase with the decreasing of hydraulic diameter, although tube D is higher than tube E heat transfer coefficient, despite having larger hydraulic diameter, suggesting hydraulic diameter alone is not the only geometrical feature that is important toward heat transfer. Literature survey of heat transfer investigation using multiport mini-channel evaporator types was performed to compare against the current trend with past trend. Yun et al. [8] commented that decreasing the hydraulic diameter was found to increase the overall heat transfer coefficient. However, Yun [10], claimed the enhancement of heat transfer was found with the increasing of internal perimeter. Additionally, Al-Zaidi et al [11] comments that for rectangular mini-channel, increase the aspect ratio also increase heat transfer coefficient. This explain why despite having larger hydraulic diameter, tube D heat transfer coefficient than tube E.

3.2. Evaluation of existing correlation

The current experimental database was compared against various correlations in literature. In 2015, Shah [12] presented a simple method of correcting the heat transfer coefficient of zeotropic mixture when applying correlation of pure fluid. The database is compared against the heat transfer coefficient correlation in its original form and its modified form.

The comparison result is shown in table 3

Table 2. Performance of existing correlation

Correlation	MAD (%)		MSE (%)	
	Original	Modified	Original	Modified
Bertsch et al. [13]	82.5	24.5	68.9	-19.4
Grungor&Winterton [14]	40.2	26.7	40	25.7
Kim & Mudawar [15]	28.7	19.2	22.4	7.8
Saitoh et al. [16]	25.5	18.3	6.4	18.6

As it is shown, the heat transfer coefficient database is relatively well predicted by the current database, and improvement upon original was observed, with the most spectacular improvement from the model of the Bertsch [13]. Although they are well predicted, it is preferable to introduce an optimized correlation for the best prediction of the present database for the more precision design of heat exchanger. In addition, since the Shah [12] method was found to made improvement to original prediction, this method is also employed during the development of correlation.

3.3. Correlation proposal

Enhancement and suppression factor can be proposed by optimizing the coefficient from the experimental data as follow:

$$E = 1 + 12000Bo^{1.5} + 0.9X_{tt}^{-0.85} \quad (14)$$

$$S = \frac{1}{1+1.1Re_l^{0.5}F^{1.15}10^{-6}} \quad (15)$$

With the nucleate boiling and single phase liquid heat transfer coefficient both used the common equations of Cooper and Dittius-Boelter respectively

$$h_{nb} = 55M^{-0.5}q^{-0.67}P_{red}^{0.12}(-log_{10}P_{red})^{-0.55} \quad (16)$$

$$h_l = 0.023Re_l^{0.8}Pr_l^{0.4}\frac{k_l}{d_h} \quad (17)$$

The evaluation was done with MAD and MAE as previously and shown the new correlation performed the best against the current experimental database.

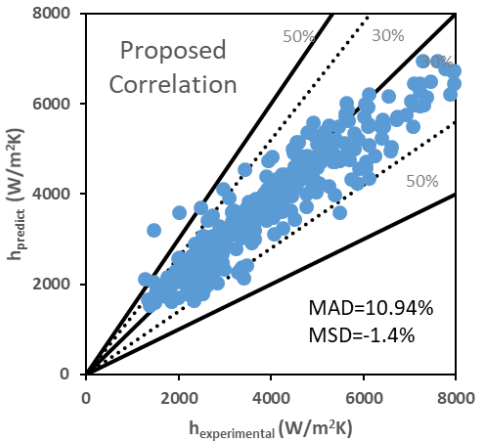

Fig. 4. Heat transfer coefficient comparison with new correlation and experimental data.

4. Conclusion

The current work investigates the heat transfer coefficient of R448A inside 3 different multiport mini-channel tube. The key findings can be summarized as follow:

1. The heat transfer coefficient is a strong function of mass flux. Heat transfer coefficient increase with increase heat flux under low mass flux conditions but display insignificant effect at higher mass flux conditions.
2. Channel geometry have important effect at lower mass flux conditions. It is found that decreasing hydraulic diameter, increasing aspect ratio (W/H), and increasing number of multiport to have favourable effect on heat transfer coefficient.
3. Past correlation can provide a reasonable prediction against the current database, with modification to account for temperature glide effect can reduce the error further. A new correlation is proposed which achieved a good accuracy with present data.

Acknowledgements

This work is supported by a National Research Foundation of Korea (NRF) grant funded by the Korea government (MSIT) (No. NRF-2020R1A2C1010902).

Nomenclature

A	: Area [m^2]	Y	: Bell-Ghaly term
B	: Scaling factor (in Thome-Shakir model)	z	: Distance from the inlet [m]
C_{pv}	: Vapor phase specific heat [kJ/kgK]	Greek letter	
C_{pl}	: Liquid phase specific heat [kJ/kgK]	β	: Liquid mass transfer coefficient (=0.0003) [m/s]
d_h	: Hydraulic diameter [m]	Δ	: Difference
E	: Convective boiling enhancement factor	μ	: Viscosity
F_{TS}	: Thome-Shakir factor	ρ	: Density
G	: Mass flux [kg/ m^{2}s]	Suscript:	
h	: Heat transfer coefficient [kW/ m^{2}K]	cb	: Convective boiling
i	: Specific enthalpy [kJ/kg]	io	: Liquid/vapor only (i=l/v)
i_{lv}	: Latent heat of vaporization [kJ/kg]	$pred$	: Predicted
k	: Thermal conductivity [W/mK]	exp	: Experimental
m	: Mass flow rate [kg/s]	ext	: External
M	: Molar mass [kg/kmol]	$glide$	: Glide (temperature)
MAD	: Mean Absolute Deviation [%]	in	: Inlet
MSE	: Mean Signed Deviation [%]	int	: Internal
P	: Pressure [kPa]	l	: Liquid phase
P_{crit}	: Critical pressure [kPa]	nb	: Nucleate Boiling
Pr	: Prandtl number	out	: Outlet
p_{tube}	: Tube perimeter [m]	$pool$	: Pool boiling
q	: Heat Flux [kW/m^2]	ref	: Refrigerant
Re	: Reynolds number	sat	: Saturated
S	: Suppression factor of Nucleate boiling	v	: Vapor phase
T	: Temperature [K], [^{o}C]	$water$	: Water
u	: Uncertainty		
x	: Vapor quality		

References

[1] A. Mota-Babiloni, J. Navarro-Esbrí, B. Peris, F. Molés, and G. Verdú, "Experimental evaluation of R448A as R404A lower-GWP alternative in refrigeration systems," *Energy Convers. Manag.*, vol. 105, pp. 756–762, Nov. 2015, doi: 10.1016/j.enconman.2015.08.034.

[2] A. Mota-Babiloni, J. Navarro-Esbrí, Á. Barragán, F. Molés, and B. Peris, "Theoretical comparison of low GWP alternatives for different refrigeration configurations taking R404A as baseline," *Int. J. Refrig.*, vol. 44, pp. 81–90, Aug. 2014, doi: 10.1016/j.ijrefrig.2014.04.015.

[3] G. Lillo, R. Mastrullo, A. W. Mauro, F. Pelella, and L. Viscito, "Experimental thermal and hydraulic characterization of R448A and comparison with R404A during flow boiling," *Appl. Therm. Eng.*, vol. 161, p. 114146, Oct. 2019, doi: 10.1016/j.applthermaleng.2019.114146.

[4] C.-H. Kim and N.-H. Kim, "Evaporation heat transfer and pressure drop of the interim (R-448A, R-449A) and long term (R-455A, R-454C) low GWP R-404A alternative refrigerants in a smooth tube," *Int. J. Heat Mass Transf.*, vol. 181, p. 121903, Dec. 2021, doi: 10.1016/j.ijheatmasstransfer.2021.121903.

[5] C.-H. Kim and N.-H. Kim, "Evaporation heat transfer and pressure drop of low GWP R-404A alternative refrigerants in a multiport tube," *Int. J. Heat Mass Transf.*, vol. 184, p. 122386, Mar. 2022, doi: 10.1016/j.ijheatmasstransfer.2021.122386.

[6] M. Li, C. Dang, and E. Hihara, "Flow boiling heat transfer of HFO1234yf and R32 refrigerant mixtures in a smooth horizontal tube: Part I. Experimental investigation," *Int. J. Heat Mass Transf.*, vol. 55, no. 13, pp. 3437–3446, Jun. 2012, doi: 10.1016/j.ijheatmasstransfer.2012.03.002.

[7] A. Berto, M. Azzolin, S. Bortolin, C. Guzzardi, and D. Del Col, "Measurements and modelling of R455A and R452B flow boiling heat transfer inside channels," *Int. J. Refrig.*, vol. 120, pp. 271–284, Dec. 2020, doi: 10.1016/j.ijrefrig.2020.08.007.

[8] R. Yun, Y. Kim, and M. S. Kim, "Convective boiling heat transfer characteristics of CO2 in microchannels," *Int. J. Heat Mass Transf.*, vol. 48, no. 2, pp. 235–242, Jan. 2005, doi: 10.1016/j.ijheatmasstransfer.2004.08.019.

[9] J. Kaew-On, K. Sakamatapan, and S. Wongwises, "Flow boiling heat transfer of R134a in the multiport

minichannel heat exchangers," *Exp. Therm. Fluid Sci.*, vol. 35, no. 2, pp. 364–374, Feb. 2011, doi: 10.1016/j.expthermflusci.2010.10.007.
[10] R. Yun, J. Hyeok Heo, and Y. Kim, "Evaporative heat transfer and pressure drop of R410A in microchannels," *Int. J. Refrig.*, vol. 29, no. 1, pp. 92–100, Jan. 2006, doi: 10.1016/j.ijrefrig.2005.08.005.
[11] A. H. Al-Zaidi, M. M. Mahmoud, and T. G. Karayiannis, "Effect of aspect ratio on flow boiling characteristics in microchannels," *Int. J. Heat Mass Transf.*, vol. 164, p. 120587, Jan. 2021, doi: 10.1016/j.ijheatmasstransfer.2020.120587.
[12] M. M. Shah, "A method for predicting heat transfer during boiling of mixtures in plain tubes," *Appl. Therm. Eng.*, vol. 89, pp. 812–821, Oct. 2015, doi: 10.1016/j.applthermaleng.2015.06.047.
[13] S. S. Bertsch, E. A. Groll, and S. V. Garimella, "A composite heat transfer correlation for saturated flow boiling in small channels," *Int. J. Heat Mass Transf.*, vol. 52, no. 7, pp. 2110–2118, Mar. 2009, doi: 10.1016/j.ijheatmasstransfer.2008.10.022.
[14] K. E. Gungor and R. H. S. Winterton, "A general correlation for flow boiling in tubes and annuli," *Int. J. Heat Mass Transf.*, vol. 29, no. 3, pp. 351–358, Mar. 1986, doi: 10.1016/0017-9310(86)90205-X.
[15] S.-M. Kim and I. Mudawar, "Universal approach to predicting saturated flow boiling heat transfer in mini/micro-channels – Part II. Two-phase heat transfer coefficient," *Int. J. Heat Mass Transf.*, vol. 64, pp. 1239–1256, Sep. 2013, doi: 10.1016/j.ijheatmasstransfer.2013.04.014.
[16] S. Saitoh, H. Daiguji, and E. Hihara, "Correlation for boiling heat transfer of R-134a in horizontal tubes including effect of tube diameter," *Int. J. Heat Mass Transf.*, vol. 50, no. 25, pp. 5215–5225, Dec. 2007, doi: 10.1016/j.ijheatmasstransfer.2007.06.019.